

A ship detection model based on multi-distributions of SAR imagery

CHEN Peng^{1,2}, LIU Renyi², HUANG Weigen²

1. College of Science, Zhejiang University, Zhejiang Hangzhou 310012, China;

2. State Key Laboratory of Satellite Ocean Environment Dynamics, Second Institute of Oceanography, Zhejiang Hangzhou 310012, China

Abstract: In this paper, we propose a new ship detection model based on SAR imagery. The model uses the Pearson distribution system to simulate the backscattering distribution of ocean surface on SAR imagery. In the Pearson distribution system, four distributions including the Pearson distributions of type I (γ), III, IV (Inverse γ) and VI are employed. Using these four distributions, we build a CFAR equation. A distribution selection machine based on β plane is used to select which distribution is adopted to specified SAR imagery. We can get four equations and the threshold of gray level. Then, using the threshold, the model can find ships from SAR images. Some tests show this model working well.

Key words: SAR, ship detection, CFAR

CLC number: TP79/TN957.52

Document code: A

Citation format: Chen P, Liu R Y and Huang W G. 2010. A ship detection model based on multi-distributions of SAR imagery. *Journal of Remote Sensing*. **14**(3): 546—557

1 INTRODUCTION

CFAR technology is often used in Ship detection in SAR imagery. From published literature we can find some distributions were used in the ship detection models, such as normal distribution, K distribution, γ distribution and etc. Eldhuset (1988) used normal distribution to form a bi-window ship detection model. This model supposes that the return signal of sea clutter obeys normal distribution and uses a fixed threshold to separate the ship from sea clutter. K distribution was applied in OMW in Canada (Vachon *et al.*, 2000). Lombardo *et al.* (2001) used γ distribution in ship detection model. But after browsing hundreds of SAR imagery we find that the sea clutter distribution is varies when the wind speed of sea surface changed in different areas or different images.

We try to use a compound distribution to fit the sea clutter distribution, then, using the compound distribution to build a ship detection model. It is noticed that Ward (1981) had introduced a compound distribution model for sea clutter. The model is derived from the radar reflectivity of the resolution cell and the radar point spread function. The distribution of the intensity is obtained by

$$f_I(x) = \int_0^{+\infty} \frac{N^N}{s^N \Gamma(N)} x^{N-1} \exp\left(-\frac{Nx}{s}\right) f_s(s) ds \quad (1)$$

where: N is the number of looks of the image, S depends on the reflectivity and the radar point spread function, $I(\cdot)$ is the γ function.

For S is not observable, Quelle *et al.* (1993) proposed a set of distributions which contain U, J, and bell-shaped probability density function, and a large variety of uni-model distributions such as γ , β of the first kind, β of the second kind, inverse γ distribution, etc. So, we can base the results of Delignon, and build a new ship detection model.

2 SHIP DETECTION MODEL OF COMPOUND DISTRIBUTION

The model consists of four parts: parameter estimation module, distribution selected module, CFAR module and detection module.

2.1 Parameter estimation module

The function of parameter estimation module is estimating the skewness parameters, kurtosis parameters, and the moment of intensity of SAR imagery. Skewness and kurtosis are used to specify which distribution is selected, and the moment parameters are used to estimate the shape parameter and the scale parameter.

Let's use β_1 denote skewness parameter, β_2 denote kurtosis parameter and m_γ denote the γ order moment of S . then the estimated γ order moment is as follows:

$$m_\gamma = N^\gamma \frac{\Gamma(N)}{\Gamma(N + \gamma)} \mu_\gamma \quad (2)$$

Received: 2009-03-18; **Accepted:** 2009-07-23

Foundation: Scientific research fund of the Second Institute of Oceanography, State Oceanic Administration (No. JG0718).

First author biography: CHEN Peng (1977—), male, Associate Professor. His main research direction is microwave remote sensing of ocean. He has more than 20 papers published. E-mail: chenpeng@sio.org.cn

where: The γ th moment of the intensity μ_γ is estimated with the intensity image, N is the number of looks of the image. β_1 and β_2 are as follows:

$$\beta_1 = \frac{m_3^2}{m_2^3} \tag{3}$$

$$\beta_2 = \frac{m_4}{m_2^3} \tag{4}$$

For all distributions, a, c_1, c_2 are important to the shape parameter and the scale parameter, so these three parameters are as follows:

$$a = \frac{m_3 m_2 - 4 m_3 m_1^2 + 3 m_2^2 m_1}{2(2 m_3 m_1 + m_2 m_1^2 - 3 m_2^2)} \tag{5}$$

$$c_1 = \frac{m_3 m_2 - 2 m_3 m_1^2 + m_2^2 m_1}{2(2 m_3 m_1 + m_2 m_1^2 - 3 m_2^2)} \tag{6}$$

$$c_2 = \frac{m_3 m_2 + m_3 m_1^2 - 2 m_2^2 m_1}{2(2 m_3 m_1 + m_2 m_1^2 - 3 m_2^2)} \tag{7}$$

2.2 Distribution selected module

The function of distribution selected module is to specify one distribution used in ship detection model by the skewness parameter and kurtosis parameter. Each S distribution can be represented by a separate subspace in the β_1 (skewness) and β_2 (kurtosis) plane (Fig.1)

In the plane, the position of β_1 - β_2 appoints the distribution of the associated distribution while the γ distribution and the inverse γ distribution are represented by a line, and the β distributions are represented by an area (Delignon, 1997). So, It can be estimated that the β_1, β_2 parameters using Eq.(3) and Eq.(4). Then we can choose the corresponding distribution in the associated distribution.

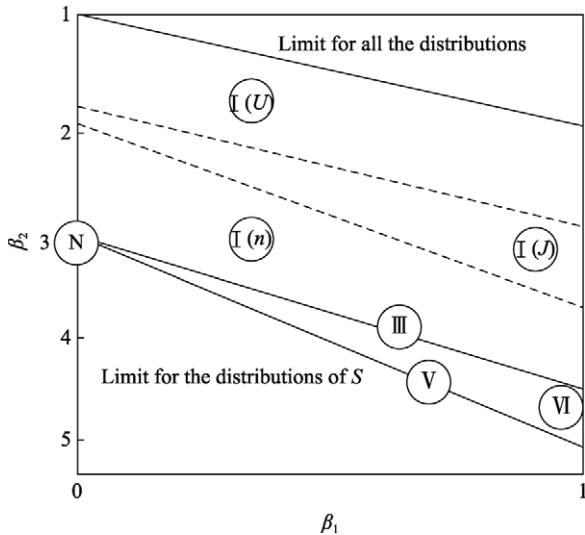


Fig. 1 S distribution in the (β_1, β_2) plane (Delignon, 1997)

N: normal distribution I: β distribution of the first kind III: γ distribution
 : inverse γ distribution : β distribution of the second kind

2.3 CFAR module

The function of CFAR module is to calculate the CFAR function and get the threshold of ship detection. For four distributions, we must form the following CFAR function.

$$CFAR = 1 - \int_{i=0}^x f_I(t) dt \tag{8}$$

where CFAR is Constant False Alarm Rate and $f(x)$ is one of four distributions.

While the distribution is β law of the first kind, its expression (Delignon, 2002) is:

$$f_I(x) = \frac{\Gamma(q)}{\Gamma(N)B(p,q)x} \left(\frac{Nx}{\beta}\right)^{(p+N-1)/2} e^{-Nx/2\beta} \times \tag{9}$$

$$W_{(-p-2q+N+1)/2, (N-p)/2} \left(\frac{Nx}{\beta}\right) \quad x \in (0, +\infty)$$

Where: $B(\cdot)$ is β function, $W(\cdot)$ is the Whittaker function, p and q are the shape parameters, β is the scaling parameter.

$$p = -\frac{a}{c_1} + 1, \quad q = \frac{a}{c_1} - \frac{1}{c_2} + 1 \tag{10}$$

$$\beta = \frac{c_1}{c_2} \tag{11}$$

While the distribution is γ law, its expression is:

$$f_I(x) = \frac{\beta}{\Gamma(N)\Gamma(\alpha)\sqrt{x}} \left(\frac{\beta\sqrt{x}}{2}\right)^{a+N-1} \times \tag{12}$$

$$K_{\alpha-N}(\beta\sqrt{x}) \quad x \in (0, +\infty)$$

where: $K(\cdot)$ is the modified Bessel function of the second kind, α is the shape parameter, β is the scaling parameter.

$$\alpha = -\frac{a}{c_1} + 1 \tag{13}$$

$$\beta = \frac{1}{c_1} \tag{14}$$

While the distribution is inverse γ law, its expression is:

$$f_I(x) = \frac{N\beta(N\beta x)^{N-1}}{B(N, \alpha)(N\beta x + 1)^{N+\alpha}} \quad x \in (0, +\infty) \tag{15}$$

where α is the shape parameter, β is the scaling parameter.

$$\alpha = -\frac{a}{c_1} + 1 \tag{16}$$

$$\beta = \frac{c_2}{a} \tag{17}$$

While the distribution is β law of the second kind, its expression is:

$$f_I(x) = \frac{\Gamma(N+q)}{\Gamma(N)B(p,q)x} \left(\frac{Nx}{\beta}\right)^N \times \tag{18}$$

$$U_{p+q, 1-N+p} \left(\frac{Nx}{\beta}\right) \quad x \in (0, +\infty)$$

where: $B(\cdot)$ is β function, $U(\cdot)$ is the hypergeometric function, p and q are the shape parameters, β is the scaling parameter.

$$p = -\frac{a}{c_1} + 1, \quad q = \frac{1}{c_2} + 1 \quad (19)$$

$$\beta = \frac{c_1}{c_2} \quad (20)$$

where, a, c_1, c_2 are obtained by operating Eq.(5), Eq.(6) and Eq.(7).

The evaluation of precision of the distribution system was done by Delignon (1997) using Kolmogorov-Smirnov test. The test shows that distributions have a good fit to the histogram of Seasat SAR imagery.

2.4 Detection module

The function of detection module is to separate the ship pixels from sea clutter in SAR imagery. After getting the shreshold level by Eq.(8), ship detection is easy by image processing. After being divided by the shreshold, some false alarm caused by speckle noise are still retained, so we add a false alarm removing step in the process (Chen, 2005).

(1) To set the min size of the ship according the image resolution.

(2) For any candid of ship pixels, we add up all pixels of one candid ship using the area growing method and get the pixel numbers of each ship.

(3) If the pixel numbers of a candid ship is large than the number we set, this candid ship is regarded as a true ship, or else, is a false alarm.

3 SHIP DETECTION EXPERIMENT

For validating the ship detection model, we selected some SAR images to test the model's performance.

Test 1: Fig.2 is an ENVISAT ASAR image of Zhou Shan area on 24, Sep.2008.

Ship detection model does some sampling randomly for the SAR image, and the sample data is used to estimate the para-

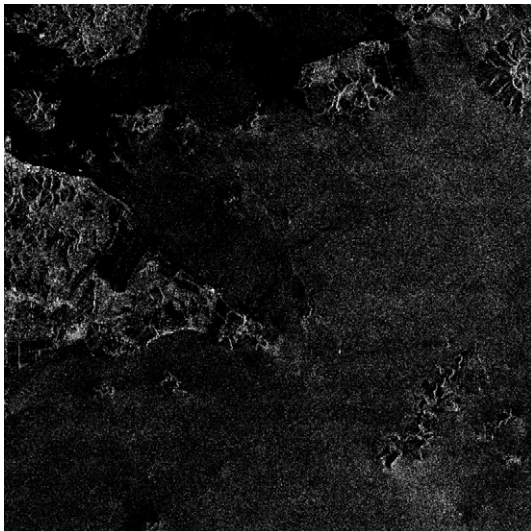


Fig. 2 ENVISAT ASAR image of Zhoushan, 24 Sep. 2008

eters. $\beta_1=1.02, \beta_2=4.08$, from the (β_1, β_2) plane, we can find that the distribution is β distribution of the first kind. The parameter $p=50, q=3, \beta=60$. Fig.3 is fitting result by the β distribution of the first kind. It can be found the line has a good fitness, especially in the tail area. We also use the other distribution to fit the histogram, Fig.4—Fig.6 is the fitting result, more errors are shown in the last three figures.

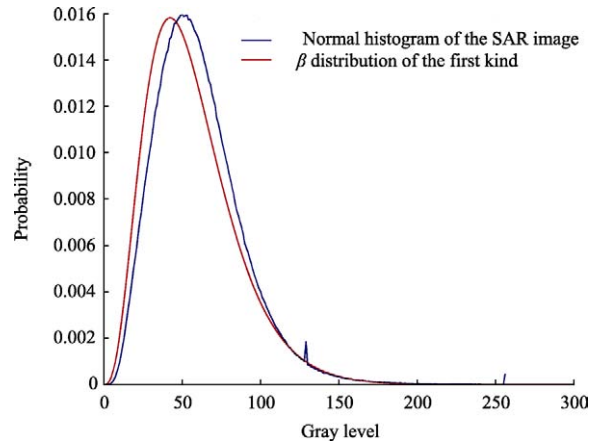


Fig. 3 Fitting result of the β distribution of the first kind

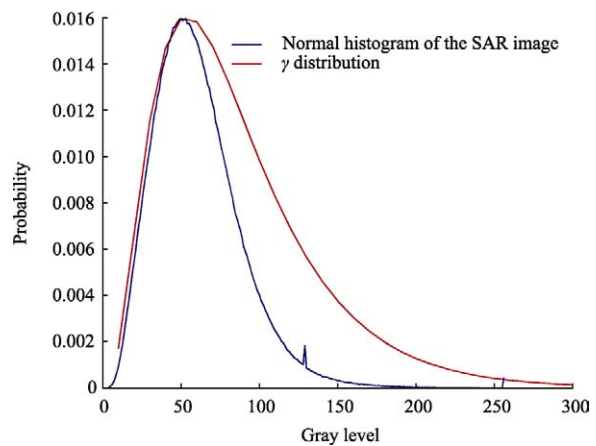


Fig. 4 Fitting result of the γ distribution

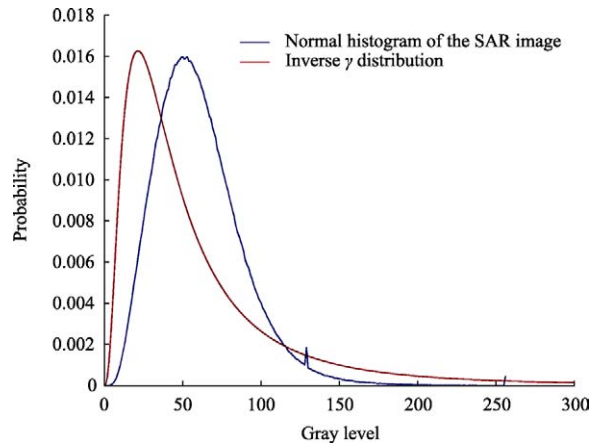


Fig. 5 Fitting result of the inverse γ distribution

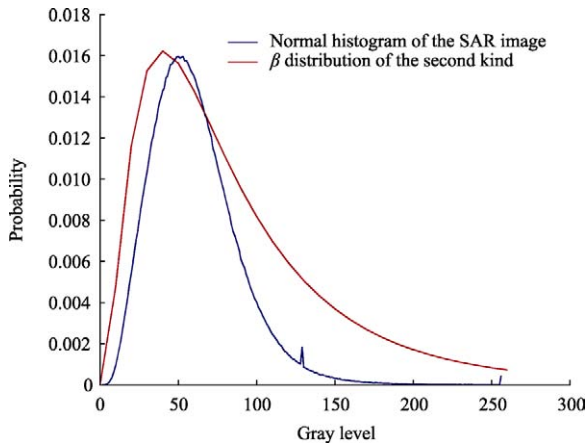


Fig. 6 Fitting result of the β distribution of the second kind

In Test 1, we denote the CFAR as 10^{-8} , and the threshold value is 201 after integral of the β distribution of the first kind. As we do not have validating data of the ship on the SAR image, the detection result is compared with the result of identification by eyes and the two results are coincidental (Fig.7).

Test 2: Fig. 8 is ENVISAT ASAR image of Wide mode at area of The Yangzi River Estuary on 16, May, 2005. The image resolution is 75 meters. After calculating, $\beta_1= 0.99$, $\beta_2= 4.5$, from the β plane, $a=0.0005$, $\beta=0.1$. Fig.9 is the fitting result of γ distribution. Though the sea back scattering is very low, the fitting result is still good.

In Test 2, we denote the CFAR as 10^{-8} , and the threshold value is 85. Fig.10 is the result of ship detection, red points are ships, and all four ships are detected correctly.



Fig. 8 ENVISAT ASAR WS mode image of Yangzi River estuary, 16 May 2005

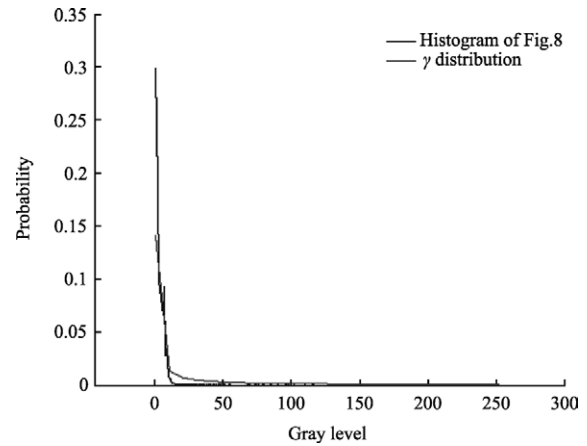


Fig. 9 Fitting result of the γ distribution

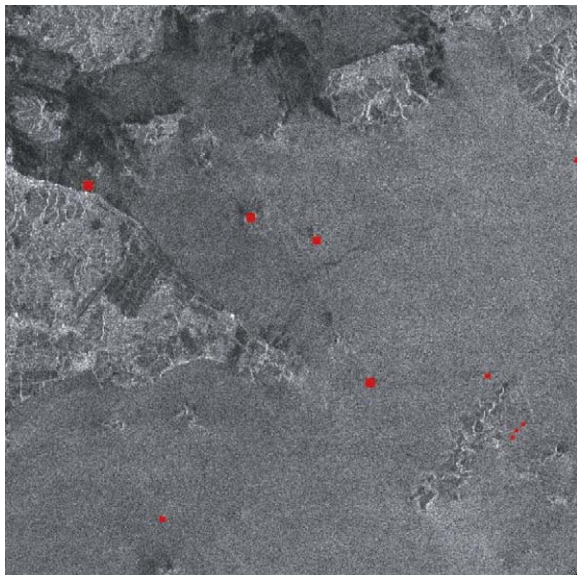


Fig. 7 Ship detection result of Fig.2 by the model

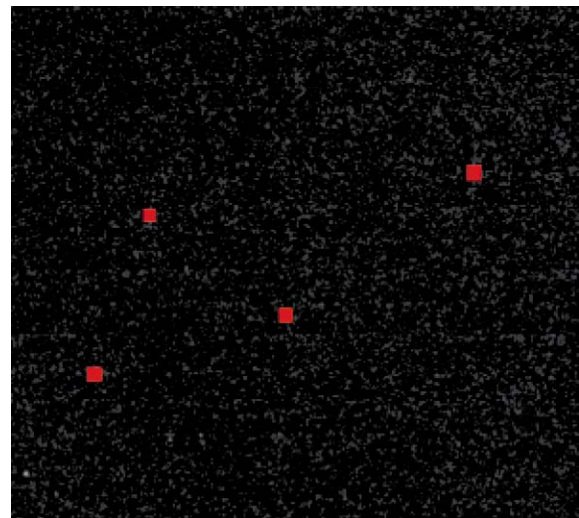


Fig. 10 Ship detection result of Fig.8 by the model

Test 3: Fig.11 is Radarsat-1 image of F2 mode at area of Zhou Shan in 29, Oct., 2005. The image resolution is 6.25 meters. After calculating, $\beta_1= 0.9$, $\beta_2= 4.8$, from the β plane, $a=4.2$, $\beta=0.05$, drops in the area of inverse γ distribution. Fig.12 is the fitting result of inverse γ distribution. The sea back scattering is very low and centralized, the fitting result is also turning up trumps.

In test 2, we denote the CFAR as 10^{-8} , and the threshold value is 48. Fig.13 is the result of ship detection, red points are ships, and all six ships are detected correctly.

Test 4: Fig.14 is ERS-2 image at the area of East China Sea on 1, jun., 2006. The image resolution is 25 meters. After calculating, $\beta_1= 0.91$, $\beta_2= 4.5$, from the β plane, $p=3.9$, $q=5.4$, $\beta=18$, drops in the area of β distribution of the second kind. Fig.15 is the fitting result of β distribution of the second kind. For ERS is VV polarization, Sea back scattering peak value is deviation to left obviously, and the fitting result is perfect.



Fig. 11 Radarsat-1 F2 mode image of Zhoushan, 29Aug. 2005

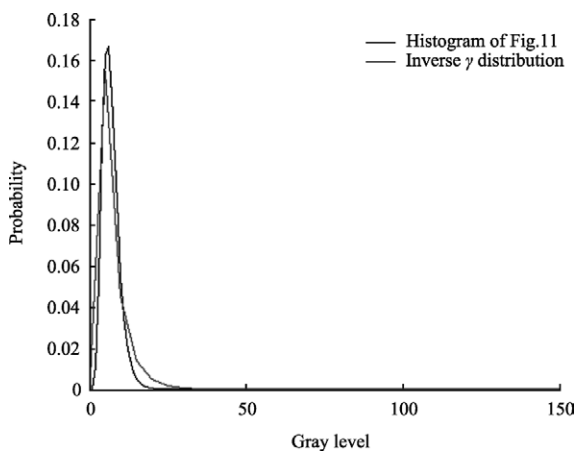


Fig. 12 Fitting result of the inverse γ distribution

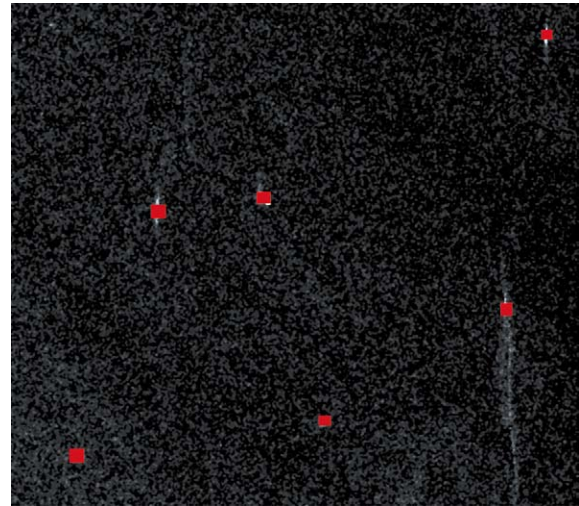


Fig. 13 Ship detection result of Fig.11 by the model

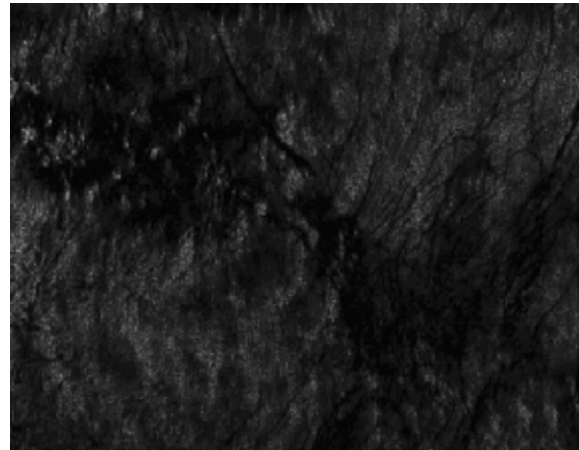


Fig. 14 ERS-2 SAR image of East Sea, 29 Jun. 2006

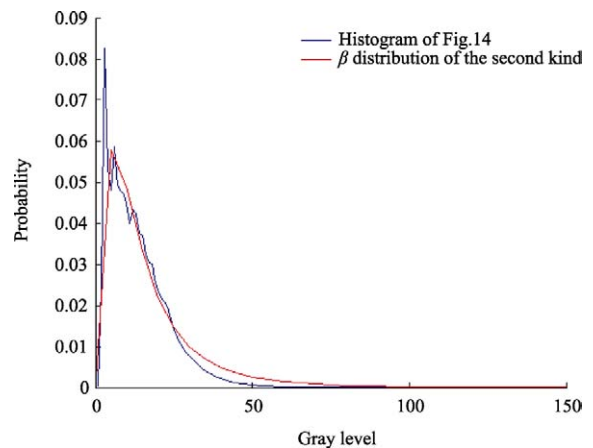


Fig. 15 Fitting result of the β distribution of the second kind

In test 4, the CFAR value is 10^{-8} , and the threshold value is 161 Fig.16 is the result of ship detection, red points are ships, and both two ships are detected correctly.

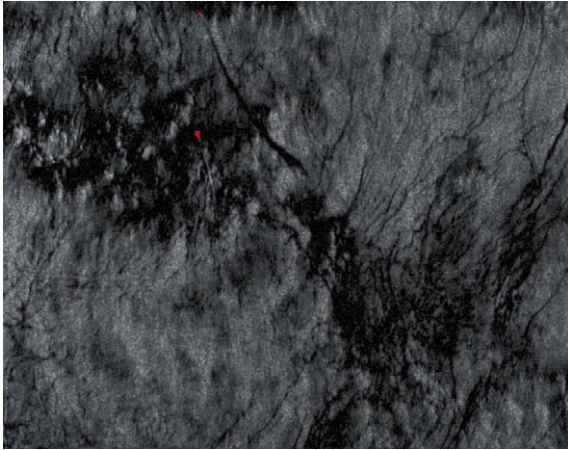


Fig. 16 Ship detection result of Fig.14 by the model

Four tests show that the model has a good adaptability for different stars and resolutions .the model has some value to further study.

4 CONCLUSION

On the basis of compound distribution system, we suggest a new ship detection model. The model applies four distributions including the β distribution of the first kind, γ distribution, inverse γ distribution and the β distribution of the second kind. We used ENVISAT ASAR, Radarsat-1 and ERS-2 SAR images to test the model, and the results show that the performance of

the model is well and further study should be done.

Acknowledgements: The authors thank the data support of China-Europe Dragon project.

REFERENCES

- Chen P, Huang W G and Yang J S. 2005. An Improved ship detection model of SAR imagery. *Journal of Remote Sensing*, **9**(3):260—264
- Delignon Y, Garelo R and Hillion A, 1997, Statistical modeling of ocean SAR images. *IEE Proc. Radar. Sonar Navig.*, **144**(6): 348—354
- Delignon Y and Pieczynski W, 2002, Modeling non-Reyleigh speckle distribution in SAR images. *IEEE Trans. Geosci. Rem. Sen.*, **40**(6): 1430—1435
- Eldhuset K. 1988. Automated ship and ship wake detection in spaceborne SAR images from coastal regions. *Proceedings of IGARSS'1988*, **3**: 1529—1533
- Lombardo P, Sciotti M and Kaplan L M. 2001. SAR prescreening using both target and shadow information. *IEEE National Radar Conference - Proceedings 2001*
- Quelle H C, Delignon Y and Marzouki A. 1993. Unsupervised Bayesian segmentation of SAR images using the pearson system distributions. *IGASS'93*. Tokyo
- Vachon P W, Thomas S J, Cranton J and Edel H R. 2000. Validation of ship detection by the ADARSAT synthetic aperture radar and the Ocean Monitoring Workstation. *Canadian Journal of Remote Sensing*, **26**(3): 200—212
- Ward K D. 1981. Compound representation of high resolution sea clutter. *Electron. Lett.*, **17**: 561—563

SAR 图像复合分布船只检测模型

陈 鹏^{1,2}, 刘仁义¹, 黄韦良²

1. 浙江大学 理学院, 浙江 杭州 310012;

2. 卫星海洋环境动力学国家重点实验室, 国家海洋局第二海洋研究所, 浙江 杭州 310012

摘 要: 提出了一种基于复合参数分布的 SAR 图像船只检测模型。模型使用 Pearson 分布系统模拟 SAR 图像海洋背景散射分布, Pearson 分布系统由 4 种参数分布组成, 包括 Pearson I 分布(γ)、III 分布、IV 分布(反 γ)和 VI 分布。模型采用基于 β 平面的分布选择器确定采用哪种分布来拟合 SAR 图像海面后向散射分布, 同时利用 4 种分布, 结合 CFAR 技术, 建立 CFAR 方程, 通过解算方程得到检测阈值, 利用阈值进行 SAR 图像船只检测。通过图像试验验证表明, 该模型检测效果良好, 具有一定的实用价值。

关键词: SAR, 参数分布, 船只, 检测

中图分类号: TP79/TN957.52

文献标识码: A

引用格式: 陈 鹏, 刘仁义, 黄韦良. 2010. SAR 图像复合分布船只检测模型. 遥感学报, 14(3): 546—557

Chen P, Liu R Y and Huang W G. 2010. A ship detection model based on multi-distributions on SAR imagery. *Journal of Remote Sensing*, 14(3): 546—557

1 引 言

参数分布结合恒虚警技术常用于 SAR 图像船只检测。从文献上发现一些常用的参数分布用于船只检测, 包括正态分布、K 分布、 γ 分布等。挪威的 Eldhuset(1988)利用正态分布建立了最早的 SAR 图像船只检测模型——双参数模型, 该模型假定 SAR 海面回波信号符合正态分布, 以一个固定的阈值作为区分船只信号与海面回波信号的标准, 实现了船只检测; 1995 年, 加拿大的海洋监测工作站(OMW)则利用 K 分布开发了用于 Radarsat SAR 图像的船只检测模块(vachon 等, 2000); 2001 年 Lombardo 等(2001)利用 γ 分布开发了一个船只检测模型。这些模型一个共同之处就是采用单一的参数分布模型, 但是经过对大量 SAR 图像的分析后, 发现海面的散射分布在同一幅图像的不同区域或者不同的图像上有不同的后向散射分布, 呈现出多样化的不规则分布, 影响原因广泛, 包括风速条件、潮流、SAR 的入射角和成像极化条件等。鉴于这种变化, 本文尝试采

用一种复合分布系统模拟海面散射分布, 进而结合 CFAR 技术建立一个新的 SAR 图像船只检测模型。早在 1981 年 Ward(1981)介绍过一个复合参数模型用于 SAR 海面杂波模拟, 模型由雷达点扩散函数导出。用于模拟海面背景的参数分布由式(1)获得。

$$f_I(x) = \int_0^{+\infty} \frac{N^N}{s^N \Gamma(N)} x^{N-1} \exp\left(-\frac{Nx}{s}\right) f_s(s) ds \quad (1)$$

N 是 SAR 图像视数, S 与雷达点扩散方程相关, $\Gamma(\cdot)$ 是 γ 方程。由于 S 难以获得, Quelle 等(1993)提出了采用 γ 、一类 β 分布、反 γ 分布和二类 β 分布等 4 种参数分布来组建复合参数模型模拟海面背景杂波, 在 Seasat SAR 图像的模拟试验表明该模型具有良好的模拟精度。本文利用 Quelle 等的研究结果, 结合 CFAR 技术, 构建一个新的基于复合参数分布的船只检测模型。

2 检测模型

基于复合参数分布的 SAR 图像船只检测模型由

收稿日期: 2009-03-18; 修订日期: 2009-07-23

基金项目: 国家海洋局第二海洋研究所基本科研业务资金项目(编号: JG0718)。

第一作者简介: 陈 鹏(1977—), 男, 湖南安仁人。2000 年获得武汉大学遥感信息工程学院摄影测量与遥感专业工学学士, 2004 年获得国家海洋局海洋动力过程与卫星海洋学重点实验室理学硕士。目前是卫星海洋环境动力学国家重点实验室副研究员, 浙江大学理学院博士研究生, 研究方向: 遥感与 3S 集成技术、海洋微波遥感。E-mail: chenpeng@sio.org.cn。

参数估计模块、分布选择模块、CFAR 解算模块和检测模块等 4 个部分组成。

2.1 参数估计模块

参数估计模块的功能是通过 SAR 图像的散射分布统计, 获取 Skewness、Kurtosis 参数和矩。Skewness 和 Kurtosis 用于参数分布选择模块, 矩用于估计特定分布的形状参数和尺度参数。本文采用 β_1 表示 Skewness 参数, β_2 表示 Kurtosis 参数, m_γ 表示 γ 阶矩。按照矩的定义, m_γ 由式(2)获得:

$$m_\gamma = N^\gamma \frac{\Gamma(N)}{\Gamma(N+\gamma)} \mu_\gamma \quad (2)$$

式中, μ_γ 为 SAR 幅度图像上获得的 γ 阶幅度矩; N 是 SAR 图像视数。 β_1 和 β_2 由式(3)和式(4)给出。

$$\beta_1 = \frac{m_3^2}{m_2^3} \quad (3)$$

$$\beta_2 = \frac{m_4}{m_2^3} \quad (4)$$

对于复合分布中任意分布, a, c_1, c_2 是重要的形状参数和尺度参数, 3 个参数由矩获得, 如式(5)一式(7)所示。

$$a = \frac{m_3 m_2 - 4 m_3 m_1^2 + 3 m_2^2 m_1}{2(2 m_3 m_1 + m_2 m_1^2 - 3 m_2^2)} \quad (5)$$

$$c_1 = \frac{m_3 m_2 - 2 m_3 m_1^2 + m_2^2 m_1}{2(2 m_3 m_1 + m_2 m_1^2 - 3 m_2^2)} \quad (6)$$

$$c_2 = \frac{m_3 m_2 + m_3 m_1^2 - 2 m_2^2 m_1}{2(2 m_3 m_1 + m_2 m_1^2 - 3 m_2^2)} \quad (7)$$

2.2 分布选择模块

分布选择模块的功能是指定某种参数分布用于船只检测。分布选择模块主要通过 Skewness 和 Kurtosis 参数确定用于检测的分布。每一个 S 型分布可以对应 Skewness 和 Kurtosis 参数平面内的一块区域, 如图 1。

在 β 平面内 $\beta_1 - \beta_2$ 指定了复合分布的类型 (Delignon & Pieczynski, 1997), 通过估计得到 β_1 和 β_2 , 采用一个简单的点与面的关系就可以确定分布类型。

2.3 CFAR 模块

CFAR 模块的功能主要是解算 CFAR 方程, 获得船只检测的阈值, 对于 4 种分布, 有式(8)的 CFAR 方程成立。

$$CFAR = 1 - \int_{i=0}^x f_I(t) dt \quad (8)$$

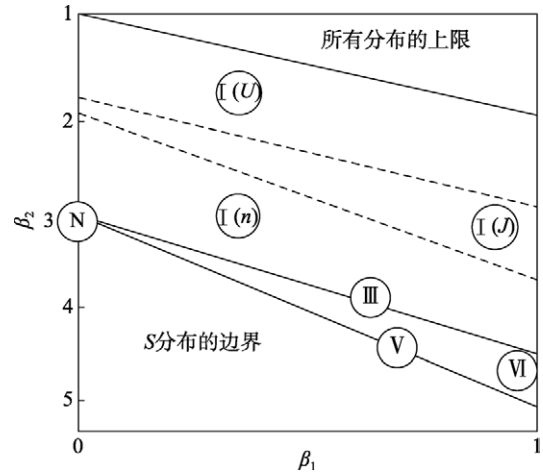


图 1 复合分布系统在 β 平面上的划分 (Delignon & Pieczynski, 1997)

N: 正态分布; I: 一类 β 分布; III: γ 分布; V: 反 γ 分布; VI: 二类 β 分布

式中, $f(x)$ 为分布之一, CFAR 为恒虚警率。

当 $f(x)$ 为一类 β 分布时, 其表达式为式(9) (Delignon & Pieczynski, 2002)。

$$f_I(x) = \frac{\Gamma(q)}{\Gamma(N)B(p, q)x} \left(\frac{Nx}{\beta}\right)^{(p+N-1)/2} e^{-Nx/2\beta} \times \quad (9)$$

$$W_{(-p-2q+N+1)/2, (N-P)/2} \left(\frac{Nx}{\beta}\right) \quad x \in (0, +\infty)$$

式中, $B(\cdot)$ 是 β 方程, $W(\cdot)$ 是 Whittaker 方程, p 和 q 是形状参数, β 是尺度参数, 如式(10)一式(11)所示。

$$p = -\frac{a}{c_1} + 1, \quad q = \frac{a}{c_1} - \frac{1}{c_2} + 1 \quad (10)$$

$$\beta = \frac{c_1}{c_2} \quad (11)$$

当 $f(x)$ 为 γ 分布时, 其表达式为式(12)。

$$f_I(x) = \frac{\beta}{\Gamma(N)\Gamma(\alpha)\sqrt{x}} \left(\frac{\beta\sqrt{x}}{2}\right)^{a+N-1} \times \quad (12)$$

$$K_{\alpha-N}(\beta\sqrt{x}) \quad x \in (0, +\infty)$$

$K(\cdot)$ 为二阶修正贝赛尔函数, α 是形状参数, β 是尺度参数, 由式(13)一式(14)获得。

$$\alpha = -\frac{a}{c_1} + 1 \quad (13)$$

$$\beta = \frac{1}{c_1} \quad (14)$$

当 $f(x)$ 为反 γ 分布时, 其表达式为式(15)。

$$f_I(x) = \frac{N\beta(N\beta x)^{N-1}}{B(N, \alpha)(N\beta x + 1)^{N+\alpha}} \quad x \in (0, +\infty) \quad (15)$$

α 是形状参数, β 是尺度参数, 由式(16)一式(17)获得。

$$\alpha = -\frac{a}{c_1} + 1 \tag{16}$$

$$\beta = \frac{c_2}{a} \tag{17}$$

当 $f(x)$ 为二类 β 分布时, 其表达式为式(18)。

$$f_I(x) = \frac{\Gamma(N+q)}{\Gamma(N)B(p,q)x} \left(\frac{Nx}{\beta}\right)^N \times U_{p+q,1-N+p} \left(\frac{Nx}{\beta}\right) \quad x \in (0, +\infty) \tag{18}$$

$B(\cdot)$ 是 β 方程, $U(\cdot)$ 是超几何方程, p 和 q 是形状参数, β 是尺度参数, 由式(19)—式(20)获得。

$$p = -\frac{a}{c_1} + 1, \quad q = \frac{1}{c_2} + 1 \tag{19}$$

$$\beta = \frac{c_1}{c_2} \tag{20}$$

式中, a, c_1, c_2 分别由式(5)、式(6) 和式(7)得到。通过解式(8)的积分方程, 可以得到检测阈值 t 。

2.4 检测模块

检测模块的功能是采用检测阈值区分船只和海面杂波, 本文采用一个简单的阈值分割实现此功能。分割完毕以后, 考虑到有些斑点噪声非常强, 可能会产生虚警, 因此在船只检测模块中增加了一个虚警去除功能(陈鹏等, 2005)。

去除虚警的步骤如下:

- (1) 根据 SAR 图像的分辨率设置船目标像元个数最小值。
- (2) 对每一个候选的可能船目标, 使用区域生长法, 统计其像元个数。
- (3) 如果像元个数的值大于或等于船目标像元个数最小值, 则认为该候选船目标为真实目标, 否则将该候选船目标作为虚警处理。

3 检测实例

为了评估该模型的有效性, 选取若干幅 SAR 图像进行了船只检测试验。图 2 是一幅舟山海域 Envisat ASAR 图像, 成像时间是 2008-09-24, 图像分辨率为 25m。

首先对图像进行采样, 通过采样数据获得: $\beta_1=1.02, \beta_2=4.08$, 从 β 平面上可知该点落在“一类 β 分布”范围内, 估算得到 $p=50, q=3, \beta=60$ 。图 3 是一类 β 分布拟合结果, 由图 3 可知, 拟合结果比较好, 除了最高峰值位置有点偏差外, 尾部有很好的近似。为了比较研究, 本文对其他 3 种分布也进行了拟合,

拟合结果见图 4—图 6, 图 4 显示 γ 分布在尾部偏差非常大, 对于船只检测是非常不利的; 图 5 在峰值和尾部有较大偏差; 图 6 在尾部也有较大偏差。

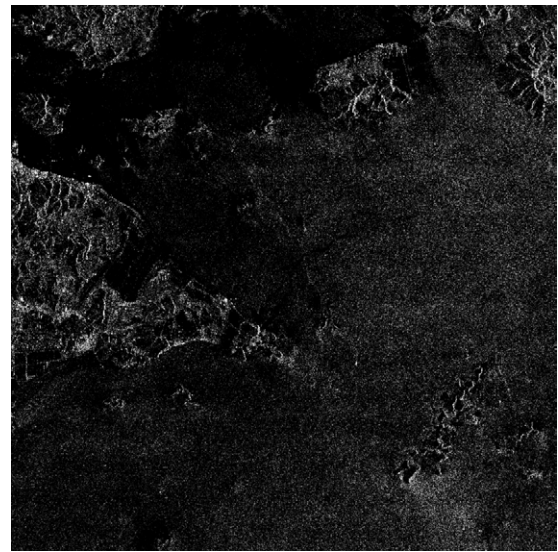


图 2 2008-09-24 舟山 ENVISAT ASAR 图像

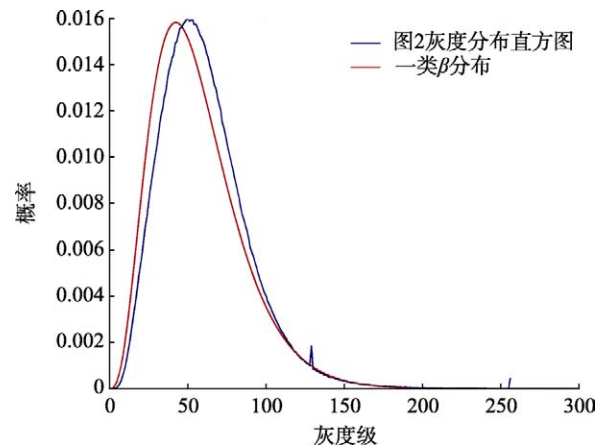


图 3 一类 β 分布拟合结果图

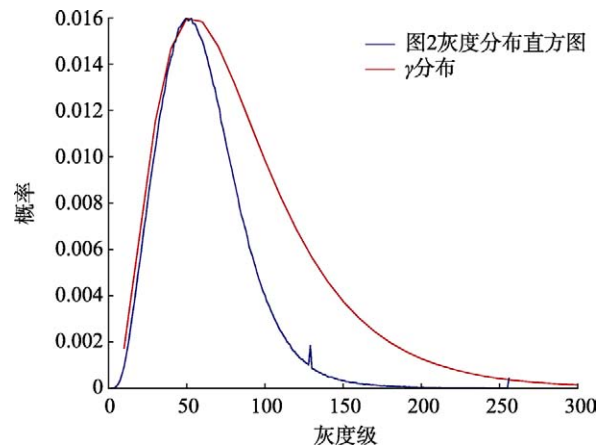


图 4 γ 分布拟合结果图

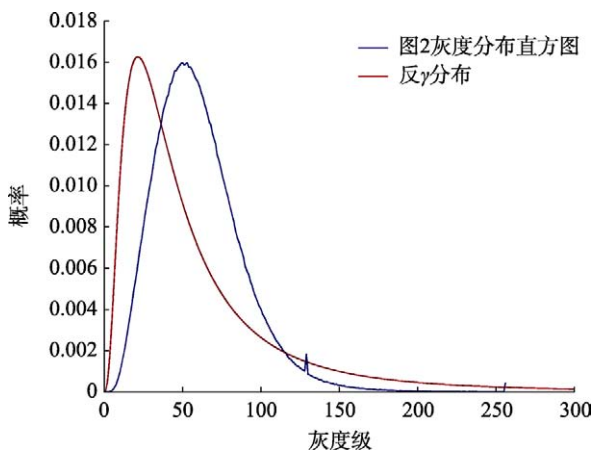


图 5 反 γ 分布拟合结果图

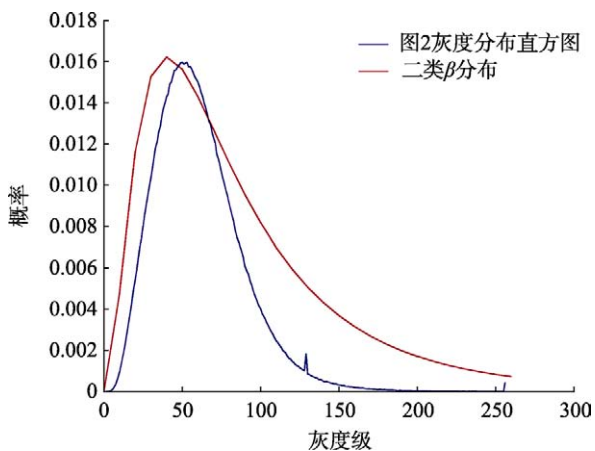


图 6 二类 β 分布拟合结果图

试验一中设定的 CFAR 值为 10^{-8} , 通过 matlab7.0 软件对一类 β 分布的积分, 计算阈值结果为 201, 检测结果如图 7, 红点为检测结果。图上共有目标 9 个, 检测结果与目视判读结果一致。

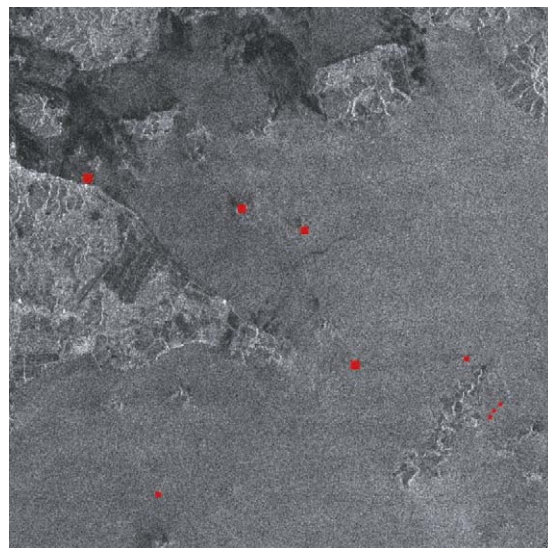


图 7 复合参数模型船只检测结果图

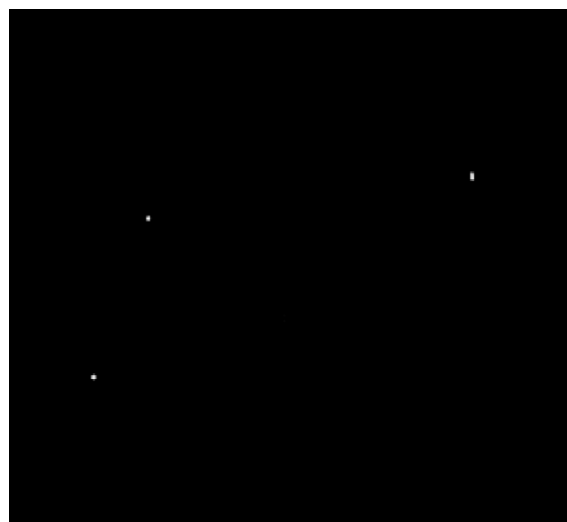


图 8 2005-05-16 长江口海域 ENVISAT ASAR WS 模式图像

图 8 是 2005-05-16 长江口某海域的 ENVISAT ASAR wide 模式图像, 图像分辨率为 75m。计算结果如下: $\beta_1=0.99, \beta_2=4.5$, 从 β 平面上可以知道该点落在“ γ 分布”范围内, $a=0.0005, \beta=0.1$ 。图 9 是 γ 分布拟合结果。由于海面背景很暗, 直方图随 x 坐标呈单边下行状态, γ 分布拟合结果与该状态一致。

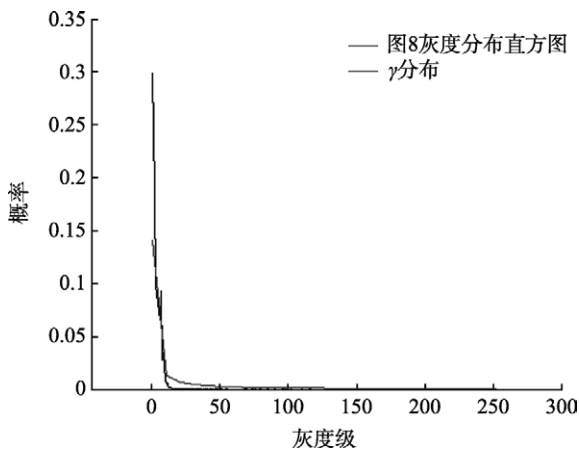


图 9 γ 分布拟合结果图

试验二中设定的 CFAR 值为 10^{-8} , 阈值计算结果为 85, 检测结果如图 10, 红点为检测结果。图上共有目标 4 个, 检测结果与目视判读结果一致。

图 11 是 2005-08-29 舟山某海域的 Radarsat-1F2 模式图像, 图像分辨率为 6.25m。计算结果如下: $\beta_1=0.9, \beta_2=4.8$, 从 β 平面上可以知道该点落在“反 γ 分布”范围内, $a=4.2, \beta=0.05$ 。图 12 是反 γ 分布拟合结果。由于成像条件的原因, Radarsat SAR 图像背景散射较暗且集中, 直方图分布集中且尖锐, 反 γ 分布拟合结果与直方图分布一致。

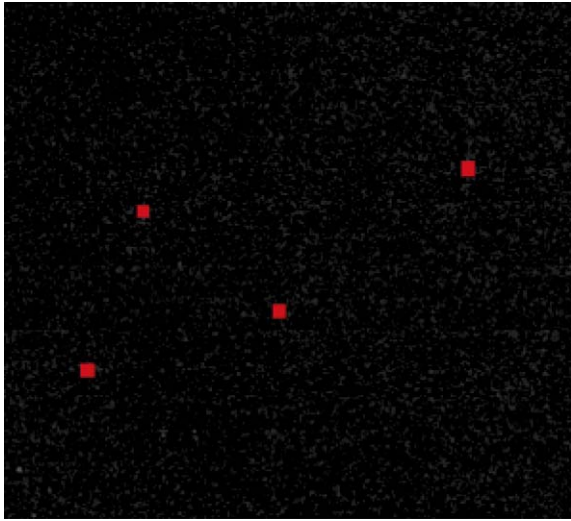


图 10 复合参数模型图 8 船只检测结果图



图 11 2005-08-29 长江口海域 Radarsat-1 F2 模式图像

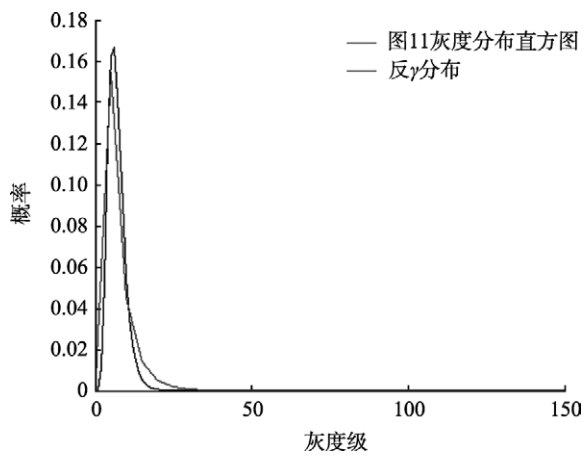


图 12 反 γ 分布拟合结果图

试验三中设定的 CFAR 值为 10^{-8} , 阈值计算结果为 48, 检测结果如图 13, 红点为检测结果。图上共有目标 6 个, 检测结果与目视判读结果一致。

图 14 是 2006-06-01 东海某海域的 ERS-2 SAR 图像, 图像分辨率为 25m。采样计算结果如下: $\beta_1=0.91, \beta_2=4.5$, 从 β 平面上可以知道该点落在“二类 β 分布”范围内, $p=3.9, q=5.4, \beta=18$ 。图 15 是二类 β 分布拟合结果。ERS-2 图像是 VV 极化方式, 直方图分布呈不规则左偏峰状态, 二类 β 分布拟合结果与直方图分布一致。

试验四中设定的 CFAR 值为 10^{-8} , 阈值计算结果为 161, 检测结果如图 16, 红点为检测结果。图 14 上有目标 2 只, 检测结果与目视判读结果一致。

4 个试验的结论表明, 该模型对不同 SAR 卫星、不同分辨率 SAR 图像有较好的适应能力, 该模型有较好的应用潜力, 值得进一步研究。

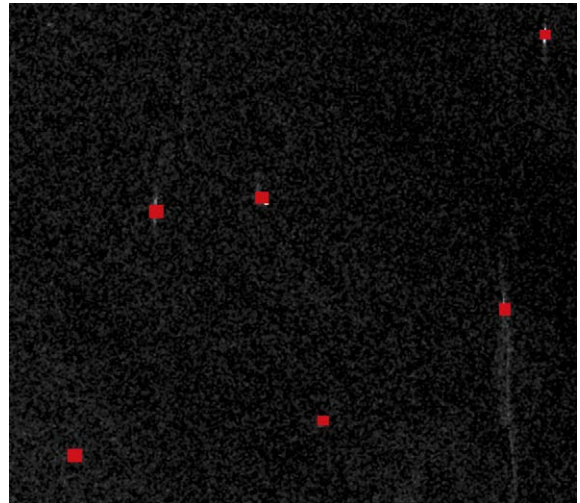


图 13 复合参数模型图 11 船只检测结果图



图 14 2000-06-01 东海海域 ERS-2 图像

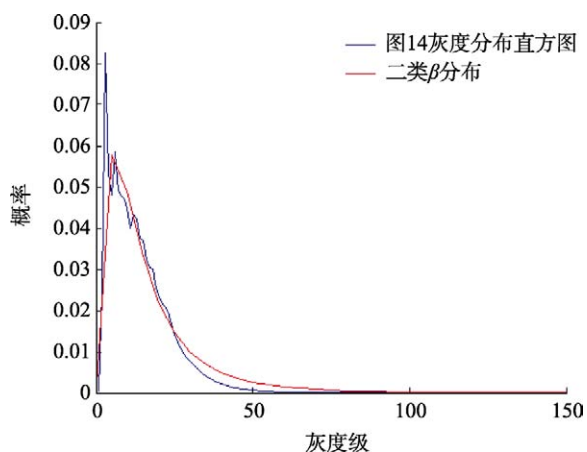
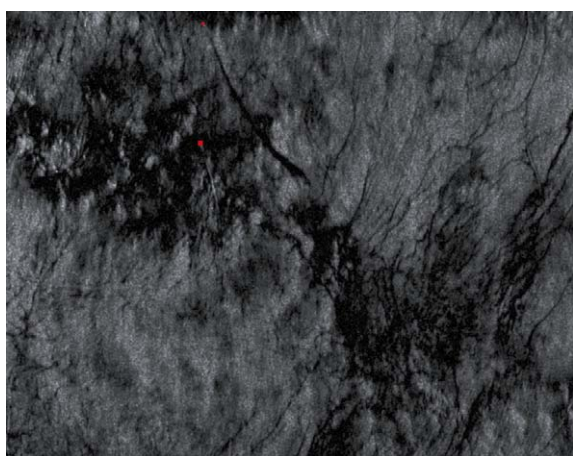
图 15 二类 β 分布拟合结果图

图 16 复合参数模型图 14 船只检测结果图

4 结 论

本文提出了一种新的基于复合参数分布的 SAR 船只检测模型。模型包含了 4 种参数分布: γ 分布、一类 β 分布、反 γ 分布和二类 β 分布。模型由参数估

计模块、分布选择模块、CFAR 解算模块和检测模块 4 部分组成。使用 Envisat ASAR、Radarsat-1 和 ERS-2 等不同模式和分辨率图像对检测模型进行了检验, 检测结果与目视判读结果一致, 试验结果表明模型具有较好的研究价值。

致 谢 感谢中欧龙计划项目提供研究数据。

REFERENCES

- Chen P, Huang W G, Fu B and Shi A C. 2005. An Improved ship detection model of SAR imagy. *Journal of Remote Sensing*, **9**(3):260—264
- Delignon Y, Garello R and Hillion A, 1997, Statistical modeling of ocean SAR images. *IEE Proc. Radar. Sonar Navig.*, **144**(6): 348—354
- Delignon Y and Pieczynski W, 2002, Modeling non-Reyleigh speckle distribution in SAR images. *IEEE Trans. Geosci. Rem. Sen.*, **40**(6): 1430—1435
- Eldhuset K. 1988. Automated ship and ship wake detection in spaceborne SAR images from coastal regions. Proceedings of IGARSS'1988, **3**: 1529—1533
- Lombardo P, Sciotti M and Kaplan L M. 2001. SAR prescreening using both target and shadow information. IEEE National Radar Conference - Proceedings 2001
- Quelle H C, Delignon Y and Marzouki A. 1993. Unsupervised Bayesian segmentation of SAR images using the pearson system distributions. IGASS'93. Tokyo
- Vachon P W, Thomas S J, Cranton J and Edel H R. 2000. Validation of ship detection by the ADARSAT synthetic aperture radar and the Ocean Monitoring Workstation. *Canadian Journal of Remote Sensing*, **26**(3): 200—212
- Ward K D. 1981. Compound representation of high resolution sea clutter. *Electron. Lett.*, **17**: 561—563

附中文参考文献

- 陈鹏, 黄韦良, 傅斌, 史爱琴. 2005. 一种改进的 CFAR 船只探测算法. *遥感学报*, **9**(3) 260—264